

# Chapter 6

## The Kinematics of 3-D Cable-Towing Systems

Qimi Jiang and Vijay Kumar

### 6.1 Introduction

Helicopters are used to transport payloads suspended via cables to hard-to-access environments in emergency response, construction, mining and military operations [1, 6, 20]. The dynamics and stability of aerial towed-cable-body systems are discussed in [20] and the trajectory control for a payload suspended from a cable from a helicopter is analyzed in [14]. In this chapter, we are interested in the mechanics of payloads suspended by multiple cables in three dimensions. The case with six cables with stationary anchors is addressed in the literature on cable-actuated platforms [5, 19]. Indeed the kinematic analysis has much in common with the analysis of cable-actuated parallel manipulators in three dimensions [2, 4, 5]. However, the key difference is that the payload pose in our case is determined by the robots' positions and the payload pose in parallel mechanisms is realized by changing the lengths of multiple cables.

When the number of cables is reduced from six to five, the conditions for equilibrium become more interesting. If the line vectors are linearly independent and the cables are taut, the line vectors and the gravity wrench axis must belong to the same linear complex [7]. The payload is free to instantaneously twist about the reciprocal screw axis. With four cables, under similar assumptions on linear independence and positive tension, the line vectors and the gravity wrench must belong to the same linear congruence. The unconstrained freedoms correspond (instantaneously) to a set of twists whose axes lie on a cylindroid. In the three-cable case, all three cables and the gravity wrench axis must lie on the same regulus—the generators of a hyperboloid which is a ruled surface [16]. Of course, in all of these cases there are special

---

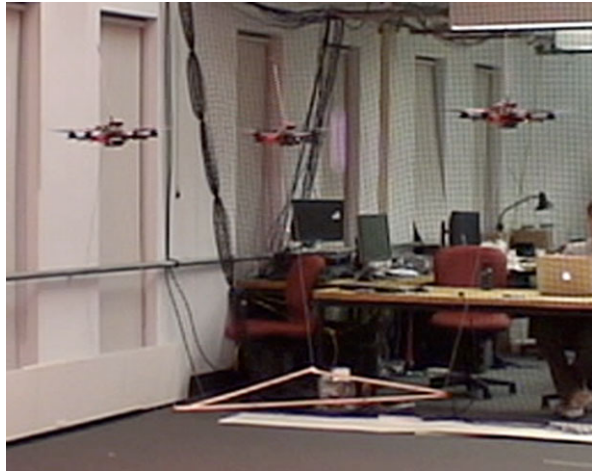
Q. Jiang (✉)

Automation Specialist, Mining Technologies International Inc., Greater Sudbury, Ontario, Canada  
e-mail: [qimi.jiang@mti.ca](mailto:qimi.jiang@mti.ca)

V. Kumar

Department of Mechanical Engineering, University of Pennsylvania, Philadelphia, PA, USA  
e-mail: [kumar@seas.upenn.edu](mailto:kumar@seas.upenn.edu)

**Fig. 6.1** 3-D towing of a triangular payload with three aerial robots [13]



configurations in which the screw systems assume special forms [7]. The arguments for the single cable and the two cable cases are similar, but in these cases, the cables and the center of mass must lie on the same vertical plane for equilibrium.

In this chapter, we address the manipulation and transportation of a payload suspended from aerial robots via cables. In previous work [3, 13]<sup>1</sup> (also see Fig. 6.1) we formulated the dynamics, control and planning problems for such systems. In this chapter, we present an overview of the kinematics of 3-D aerial manipulation. We are interested in (a) the inverse kinematics problem, the problem of determining the positions of the aerial robots to which the cables are attached given the desired position and orientation of the payload suspended by cables; and (b) the direct kinematics problem, the problem of determining the position and orientation of the suspended payload for a given position of the aerial robots.

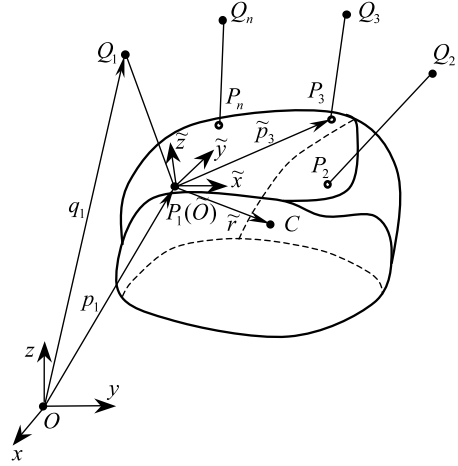
In Sect. 6.2, we formulate the conditions for static equilibrium and the geometric constraints that are at the heart of this analysis. In Sect. 6.3, we address the direct kinematics problem where we will limit ourselves to the case with vertical planes of symmetry. We show how to solve the inverse kinematics using dialytic elimination in Sect. 6.4. In Sect. 6.5 we discuss constraints on solutions imposed by limitations on cable tensions. Finally, we conclude the chapter with a few remarks about open problems in Sect. 6.7.

## 6.2 The Conditions of Equilibrium and Constraint

In Fig. 6.2 we show the general case of a payload suspended by cables from  $n$  aerial robots. Suppose that the position of robot  $Q_i$  in the inertial frame is  $\mathbf{q}_i = [x_{qi}, y_{qi}, z_{qi}]^T$ . The positions of the attachment point  $P_i$  in the inertial and body-

<sup>1</sup>Taken from [3], reprinted with kind permission © Sage 2012.

**Fig. 6.2** A payload suspended in three dimensions by multiple aerial robots



fixed frames are  $\mathbf{p}_i = [x_{pi}, y_{pi}, z_{pi}]^T$  and  $\tilde{\mathbf{p}}_i = [\tilde{x}_{pi}, \tilde{y}_{pi}, \tilde{z}_{pi}]^T$  respectively. The positions of the center of mass of the payload in the inertial and body-fixed frames are  $\mathbf{r} = [x, y, z]^T$  and  $\tilde{\mathbf{r}} = [\tilde{x}, \tilde{y}, \tilde{z}]^T$  respectively. If the length of cable  $i$  is given by  $l_i$ , the unit wrench of cable  $i$  with respect to the origin  $O$  of the inertial frame can be given as

$$\mathbf{w}_i = \frac{1}{l_i} \begin{bmatrix} \mathbf{q}_i - \mathbf{p}_i \\ \mathbf{p}_i \times \mathbf{q}_i \end{bmatrix}. \tag{6.1}$$

The wrench caused by the weight of the payload with respect to the origin  $O$  is

$$\mathbf{G} = -mg \begin{bmatrix} \mathbf{e}_3 \\ \mathbf{r} \times \mathbf{e}_3 \end{bmatrix}, \tag{6.2}$$

where  $mg$  is the weight of the payload and  $\mathbf{e}_3$  is the unit vector  $[0, 0, 1]^T$ . If the tension of cable  $i$  is given by  $T_i$ , the static equilibrium condition of the payload can be given as

$$[\mathbf{w}_1 \ \mathbf{w}_2 \ \dots \ \mathbf{w}_n] \begin{bmatrix} T_1 \\ T_2 \\ \vdots \\ T_n \end{bmatrix} + \mathbf{G} = \mathbf{0}. \tag{6.3}$$

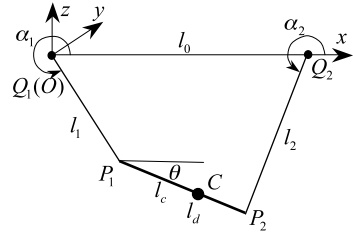
Also, the cable lengths should satisfy the following geometric constraints:

$$\|\mathbf{q}_i - \mathbf{p}_i\| = l_i \quad (i = 1, 2, \dots, n). \tag{6.4}$$

### 6.3 Direct Kinematics

This section addresses the direct kinematics problem which can be described as follows [10, 11]: *Given the positions of the aerial robots, find the possible positions and orientations of the payload, that satisfy (6.3) and (6.4).*

**Fig. 6.3** Four-bar linkage (payload suspended from two robots)



The general case with three robots was formulated in [11]. The resulting set of equations is quite unwieldy and does not lend itself to a closed form solution. For simplicity, we address the direct kinematics problem for the symmetric case here. The payload is a regular polygon suspended from  $n$  identical cables and we consider the case where the  $n$  robots form a regular polygon on a horizontal plane. The motion of such a 3-D cable system has several vertical planes of symmetry. In each plane the motion can be described in terms of the motion of an equivalent planar 4-bar linkage. Hence, an analytic algorithm based on resultant elimination can be used to determine all possible equilibrium configurations of the planar 4-bar linkage, which then offers a basis for solving the direct kinematics problem of the 3-D cable system with symmetric geometry.

We start with the planar abstraction which takes the form of a four bar linkage in Fig. 6.3, in which we assume  $Q_1$  and  $Q_2$ , the two robots, are on the same horizontal plane. The lengths of the four bars are  $|Q_1 Q_2| = l_0$ ,  $|P_1 Q_1| = l_1$ ,  $|P_2 Q_2| = l_2$ , and  $|P_1 P_2| = l_d$  respectively. The center of mass of the payload, the coupler  $P_1 P_2$ , is  $C$  and  $|P_1 C| = l_c$ . Also, the masses of the cables (the input and output bars) can be neglected. If  $Q_1$  is chosen as the origin  $O$  and  $Q_1 Q_2$  as the  $x$  axis of the frame, the coordinates of  $P_1$  and  $P_2$  can be respectively given as

$$\begin{aligned} \mathbf{p}_1 &= \mathbf{q}_1 + l_1[\cos \alpha_1, \sin \alpha_1]^T = \mathbf{q}_1 + l_1[x_1, z_1]^T, \\ \mathbf{p}_2 &= \mathbf{q}_2 + l_2[\cos \alpha_2, \sin \alpha_2]^T = \mathbf{q}_2 + l_2[x_2, z_2]^T, \end{aligned} \quad (6.5)$$

where

$$\begin{aligned} x_1^2 + z_1^2 &= 1, \\ x_2^2 + z_2^2 &= 1. \end{aligned} \quad (6.6)$$

Referring to (6.3), the equilibrium condition for the planar 4-bar linkage can be given as

$$\begin{aligned} x_1 T_1 + x_2 T_2 &= 0, \\ z_1 T_1 + z_2 T_2 + mg &= 0, \\ l_0 l_d z_2 T_2 + mg[l_1(l_d - l_c)x_1 + l_2 l_c x_2 + l_0 l_c] &= 0. \end{aligned} \quad (6.7)$$

From the third equation of (6.7), one gets

$$T_2 = -mg[l_1(l_d - l_c)x_1 + l_2 l_c x_2 + l_0 l_c]/(l_0 l_d z_2). \quad (6.8)$$

Substituting  $T_2$  into the first equation of (6.7), one gets

$$T_1 = -mg[l_1(l_d - l_c)x_1 + l_2l_cx_2 + l_0l_c]x_2/(l_0l_dx_1z_2). \quad (6.9)$$

Then, substituting  $T_1$  and  $T_2$  into the second equation of (6.7), one gets

$$\begin{aligned} & [l_1(l_c - l_d)x_1x_2 - l_2l_cx_2^2 - l_0l_cx_2]z_1 \\ & - [l_1(l_c - l_d)x_1^2 - l_2l_cx_1x_2 + l_0(l_d - l_c)x_1]z_2 = 0. \end{aligned} \quad (6.10)$$

Also, the coordinates of  $P_1$  and  $P_2$  should satisfy the geometric constraint  $|P_1P_2| = l_d$ , hence

$$l_1l_2z_1z_2 + l_1l_2x_1x_2 + l_0(l_1x_1 - l_2x_2) + g_0 = 0, \quad (6.11)$$

where

$$g_0 = [l_d^2 - l_0^2 - l_1^2(x_1^2 + z_1^2) - l_2^2(x_2^2 + z_2^2)]/2. \quad (6.12)$$

From the trigonometric identities given by (6.6), it is clear that  $g$  is a constant. Now, we have four equations consisting of (6.6), (6.10) and (6.11) in four unknowns ( $x_1, z_1, x_2, z_2$ ). In order to solve this nonlinear system, elimination algorithms are used. From (6.11), one gets

$$z_2 = -[l_1l_2x_1x_2 + l_0(l_1x_1 - l_2x_2) + g]/(l_1l_2z_1). \quad (6.13)$$

Substituting (6.13) into (6.10) and the second equation of (6.6), one gets

$$\begin{aligned} & [l_1^2l_2(l_c - l_d)x_1x_2 - l_1l_2^2l_cx_2^2 - l_1l_2l_cl_0x_2]z_1^2 + [l_1^2l_2(l_c - l_d)x_2 + l_1^2(l_c - l_d)l_0]x_1^3 \\ & + [l_0l_1l_2(2l_d - 3l_c)x_2 - l_1l_2^2l_cx_2^2]x_1^2 + l_1[(l_d - l_c)l_0^2 + (l_c - l_d)g]x_1^2 \\ & + l_2^2l_cl_0x_1x_2^2 + l_2[(l_c - l_d)l_0^2 - l_cg]x_1x_2 + (l_d - l_c)l_0gx_1 = 0, \quad (6.14) \\ & (l_1^2l_2^2x_2^2 + 2l_1^2l_2l_0x_2 + l_1^2l_0^2)x_1^2 - 2l_1l_2^2l_0x_1x_2^2 + 2l_1l_2(g - l_0^2)x_1x_2 + 2l_1l_0gx_1 \\ & + (l_1^2l_2^2x_2^2 - l_1^2l_2^2)z_1^2 + l_2^2l_0^2x_2^2 - 2l_2l_0bx_2 + g^2 = 0. \end{aligned}$$

It can be seen that there is only one quadratic term in  $z_1$  in every equation of (6.14). Referring to the first equation of (6.6),  $z_1^2$  can be substituted by  $(1 - x_1^2)$ . Hence, (6.14) becomes

$$\begin{aligned} & l_2\{2l_0l_1(l_d - l_c)x_1^2 + [(l_c - l_d)(l_0^2 + l_1^2) - l_cg]x_1 - l_1l_cl_0\}x_2 \\ & + (l_2^2l_cl_0x_1 - l_1l_2^2l_c)x_2^2 + (l_d - l_c)[-l_0l_1^2x_1^3 + l_1(l_0^2 - g)x_1^2 + l_0gx_1] = 0, \quad (6.15) \\ & l_2^2(l_0^2 + l_1^2 - 2l_1l_0x_1)x_2^2 + 2l_2[l_1^2l_0x_1^2 + l_1(g - l_0^2)x_1 - l_0g]x_2 \\ & + (l_1^2l_0^2 + l_1^2l_2^2)x_1^2 + 2l_1l_0gx_1 - l_1^2l_2^2 + g^2 = 0. \end{aligned}$$

**Table 6.1** Real solutions of the equilibrium problem of the planar 4-bar linkage shown in Fig. 6.4

No.	$x_1$	$x_2$	$z_1$	$z_2$	No.	$x_1$	$x_2$	$z_1$	$z_2$
1	0.826	0.127	0.564	0.992	9	0.332	-0.777	0.943	0.630
2	0.826	0.127	-0.564	-0.992	<b>10</b>	<b>0.332</b>	<b>-0.777</b>	<b>-0.943</b>	<b>-0.630</b>
3	0.777	-0.332	0.630	0.943	11	0.180	-0.180	0.984	0.984
<b>4</b>	<b>0.777</b>	<b>-0.332</b>	<b>-0.630</b>	<b>-0.943</b>	<b>12</b>	<b>0.180</b>	<b>-0.180</b>	<b>-0.984</b>	<b>-0.984</b>
5	0.620	-0.620	0.785	0.785	13	-1	NA	NA	NA
<b>6</b>	<b>0.620</b>	<b>-0.620</b>	<b>-0.785</b>	<b>-0.785</b>	14	-1	NA	NA	NA
7	-0.127	-0.826	0.992	0.564	15	1	2.116	0	NA
8	-0.127	-0.826	-0.992	-0.564	16	1	2.116	0	NA

In order to eliminate  $x_2$  from (6.15), the resultant algorithm is used [17]. This leads to the following 8 degree polynomial equation in  $x_1$ :

$$G_8x_1^8 + G_7x_1^7 + G_6x_1^6 + G_5x_1^5 + G_4x_1^4 + G_3x_1^3 + G_2x_1^2 + G_1x_1 + G_0 = 0, \quad (6.16)$$

where  $G_0, G_1, \dots, G_8$  are constant coefficients.

In principle, up to 8 solutions in  $x_1$  can be found from (6.16). For every solution of  $x_1$  substituted into (6.15), one corresponding solution in  $x_2$  can be obtained. Then, up to two solutions of  $z_1$  can be obtained by substituting a solution of  $x_1$  into the first equation of (6.6). Finally, a corresponding solution of  $z_2$  can be obtained by (6.13). It seems that the total number of solutions are 16. However, the computational results show that the maximal number of real solutions is no more than 12, a result that is consistent with the reasoning in [12]. This point can be demonstrated by an example for which the geometric parameters are  $l_0 = 4$  m,  $l_1 = 5$  m,  $l_2 = 5$  m,  $l_d = 2.2$  m,  $l_c = 1.1$  m,  $mg = 10$  N and the results are listed in Table 6.1.

When  $x_1 = -1$ , two real solutions (1.800, -1.124) can be obtained for  $x_2$  from the first equation of (6.15). However, no real solutions can be found for  $x_2$  from the second equation of (6.15). When  $x_1 = 1$ , the corresponding real solutions can be found for  $x_2$  and  $z_1$ , but no real solutions can be found for  $z_2$ . In other words, when  $x_1 = \pm 1$ , there is no real solutions for the problem. Hence, the total number of real solutions of the considered problem is only 12. The corresponding equilibrium configurations are shown in Fig. 6.4 in which the thick solid lines represent the coupler, the thin solid lines represent the input or output links (cables) with positive tensions, and the dashed lines represent the input or output links (cables) with negative tensions. Since cable tensions cannot be negative, only the four solutions (Nos. 4, 6, 10 and 12) listed in Table 6.1 make physical sense.

We use the methodology for determining equilibrium configurations of the planar 4-bar linkage to solve the direct kinematics problem of a homogeneous, regular, polygonal payload suspended by  $n$  identical cables with  $n$  robots forming a regular, horizontal polygon. Take the case with six robots as an example. Thus, the six aerial robots ( $Q_1, Q_2, Q_3, Q_4, Q_5, Q_6$ ) lie in the same horizontal plane and form a regular hexagon with side length  $l_q$ . The attachment points ( $P_1, P_2, P_3, P_4, P_5, P_6$ ) of the

**Fig. 6.4** Twelve equilibrium configurations of the planar 4-bar linkage

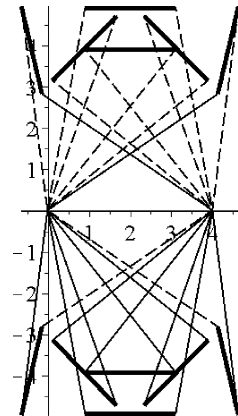
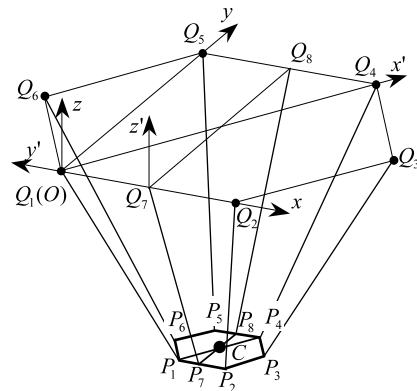


**Table 6.2** Geometric parameters of equivalent planar 4-bar linkages for case with 6 robots

No.	$l_0$	$l_1$	$l_2$	$l_d$	$l_c$
1	$2l_q$	$l$	$l$	$2l_p$	$l_p$
2	$\sqrt{3}l_q$	$\frac{\sqrt{4l^2 - (l_q - l_p)^2}}{2}$	$\frac{\sqrt{4l^2 - (l_q - l_p)^2}}{2}$	$\sqrt{3}l_p$	$\frac{\sqrt{3}l_p}{2}$

**Fig. 6.5** A homogeneous, regular polygonal payload ( $P_1 P_2 P_3 P_4 P_5 P_6$ ) suspended from six robots  $Q_1, Q_2, Q_3, Q_4, Q_5,$  and  $Q_6$  arranged on the verticals of a horizontal regular polygon



payload also form a regular hexagon with side length  $l_p$ , and the center of mass of the payload coincides with the centroid of hexagon  $P_1 P_2 P_3 P_4 P_5 P_6$ . Also, the cables have the same length  $l$ .

An equilibrium configuration for this geometry is shown in Fig. 6.5. There are six vertical planes of symmetry that fall into two classes. In the first class, every vertical plane of symmetry, e.g.,  $Q_1 P_1 P_4 Q_4$ , passes through the diagonal lines of regular hexagons  $Q_1 Q_2 Q_3 Q_4 Q_5 Q_6$  and  $P_1 P_2 P_3 P_4 P_5 P_6$ . In the second class, every vertical plane of symmetry, e.g.,  $Q_7 P_7 P_8 Q_8$ , passes through the middle points of the opposite sides of regular hexagons  $Q_1 Q_2 Q_3 Q_4 Q_5 Q_6$  and  $P_1 P_2 P_3 P_4 P_5 P_6$ . If the payload swings in one of these six vertical planes of symmetry, it is equivalent

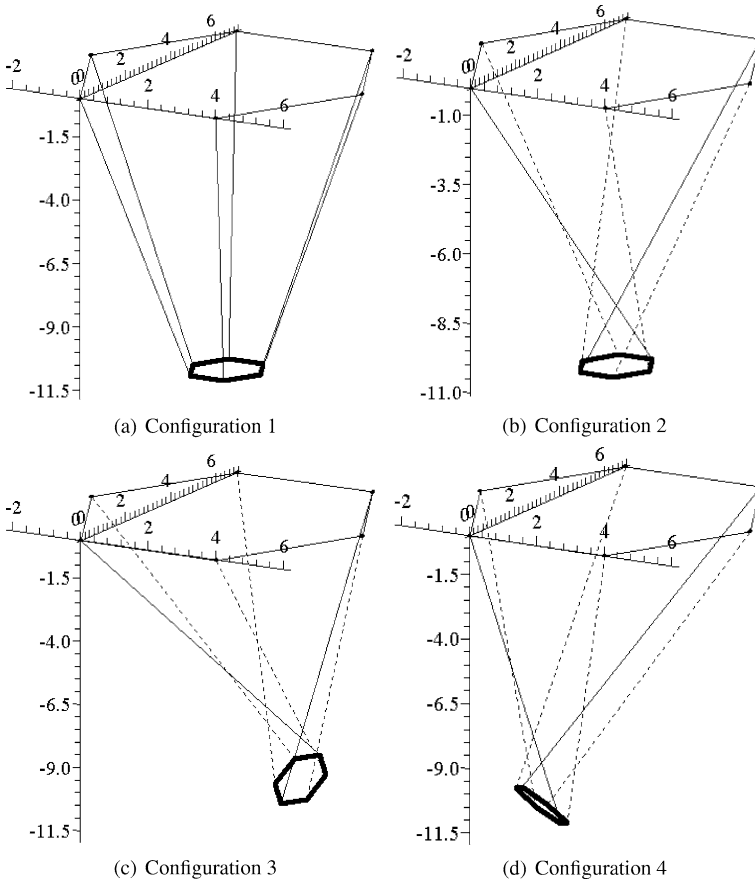


**Fig. 6.6** Four equilibrium configurations of a payload suspended from six robots determined by the equivalent planar four bar linkage in the plane  $Q_1 P_1 P_4 Q_4$

to the motion of a 4-bar linkage in the same plane. The geometric parameters of two classes equivalent planar 4-bar linkages are listed in Table 6.2.

If  $l$ ,  $l_q$  and  $l_p$  are respectively given by 12 m, 4 m and 1 m, four equilibrium configurations can be determined in every vertical plane of symmetry of the first class using the corresponding equivalent planar 4-bar linkage. Figure 6.6 shows the four equilibrium configurations in the vertical plane  $Q_1 P_1 P_4 Q_4$ . In every configuration except configuration 1 which coincides with the initial configuration, there are four cables ( $P_2 Q_2$ ,  $P_3 Q_3$ ,  $P_5 Q_5$  and  $P_6 Q_6$ ) are slack and represented by the dashed lines.

Also, four equilibrium configurations can be determined in every vertical plane of symmetry of the second class using the corresponding equivalent planar 4-bar linkage. Figure 6.7 shows the four equilibrium configurations in the vertical plane  $Q_7 P_7 P_8 Q_8$ . In every configuration except configuration 1 which coincides with the



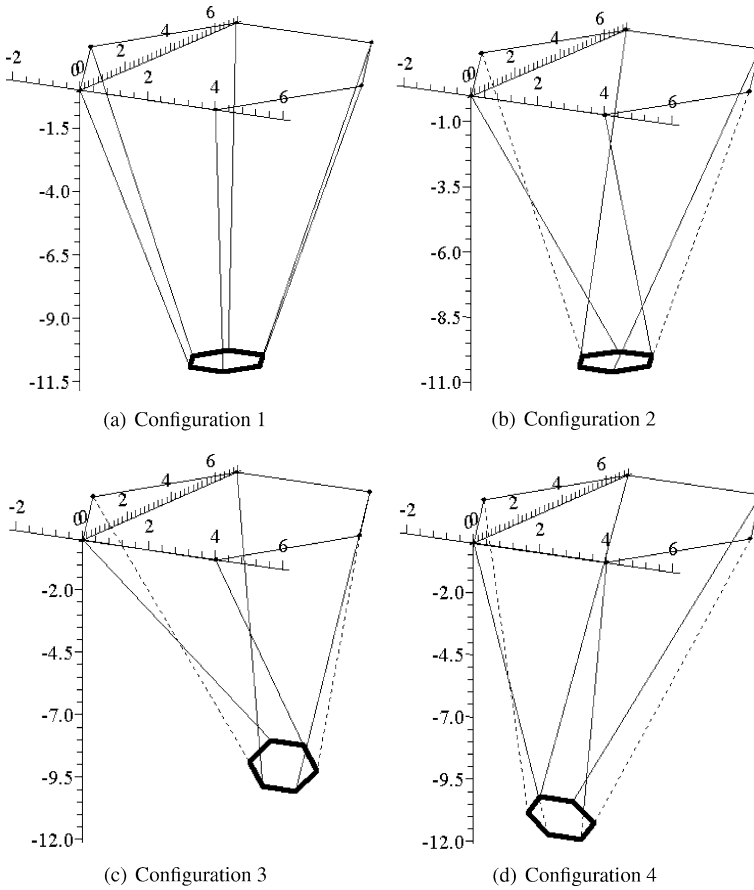


**Fig. 6.7** Four equilibrium configurations of a payload suspended from six robots determined by the equivalent planar four bar linkage in the plane  $Q_7P_7P_8Q_8$

initial configuration, there are two cables ( $P_3Q_3$  and  $P_6Q_6$ ) are slack and represented by the dashed lines.

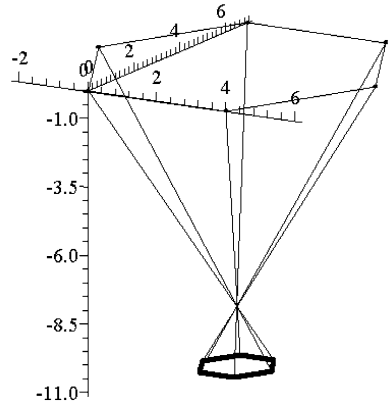
However, configurations found by the four-bar linkage abstraction are only a subset of equilibrium configurations. This is easily seen in Fig. 6.8 in which every pair opposite cables intersects. Hence, the total number of equilibrium configurations for the case with six robots is at least 20.

In [11], we provide a more exhaustive analysis of such systems by considering case studies with  $n = 3, 4, 5,$  and  $6$ .

### 6.4 Inverse Kinematics

In this section, we present an efficient analytic algorithm based on Dyalitic elimination to solve this inverse kinematics problem which can be described as follows

**Fig. 6.8** The equilibrium configuration with six robots in which every pair of opposite cables intersect each other



[8, 9]:<sup>2</sup> Given a desired position and orientation of the payload ( $\mathbf{r}, \mathbf{R}$ ), find the positions of the aerial robots ( $\mathbf{q}_i, i = 1, 2, \dots, n$ ) that satisfy (6.3) and (6.4).

To maintain a desired position and orientation, the payload needs at least three attachment points. Thus, for the cases with 1 and 2 robots, the inverse kinematics problem, in general, has no solution. However, for the cases with 3 or more robots, there are infinitely many solutions, because the number of unknowns is greater than the sum of the number of equations of static equilibrium and the number of constraints.

For the case with three robots, if the tensions  $T_i$  ( $i = 1, 2, 3$ ) of three cables are given, there are 9 unknowns ( $x_{qi}, y_{qi}, z_{qi}, i = 1, 2, 3$ ) in 9 equations given by (6.3) and (6.4). Hence, it should be possible to find a finite number of solutions for the inverse kinematics problem.

From (6.3), one gets

$$\begin{aligned}
 s_1x_1 + s_2x_2 + s_3x_3 &= 0, \\
 s_1y_1 + s_2y_2 + s_3y_3 &= 0, \\
 s_1z_1 + s_2z_2 + s_3z_3 &= mg, \\
 -s_6y_1 + s_5z_1 - s_9y_2 + s_8z_2 - s_{12}y_3 + s_{11}z_3 &= t_1, \\
 s_6x_1 - s_4z_1 + s_9x_2 - s_7z_2 + s_{12}x_3 - s_{10}z_3 &= t_2, \\
 -s_5x_1 + s_4y_1 - s_8x_2 + s_7y_2 - s_{11}x_3 + s_{10}y_3 &= 0,
 \end{aligned} \tag{6.17}$$

where  $s_1, s_2, \dots, s_{12}, t_1, t_2$  are constants or functions of  $T_i$  ( $i = 1, 2, 3$ ), and  $x_i = x_{qi} - x_{pi}, y_i = y_{qi} - y_{pi}$  and  $z_i = z_{qi} - z_{pi}$  ( $i = 1, 2, 3$ ). From (6.4), one gets

$$x_i^2 + y_i^2 + z_i^2 = l_i^2 \quad (i = 1, 2, 3). \tag{6.18}$$

<sup>2</sup>Taken from [8, 9], reprinted with kind permission © ASME 2012.

Hence, the problem reduces to solving the 9 unknowns  $(x_i, y_i, z_i, i = 1, 2, 3)$  using the 9 equations given by (6.17) and (6.18). Once  $x_i, y_i, z_i$  ( $i = 1, 2, 3$ ) are known, the position coordinates  $x_{qi}, y_{qi}, z_{qi}$  ( $i = 1, 2, 3$ ) of the robots can be easily obtained.

As long as the tensions of the cables are not zero, the six equations in (6.17) are linear independent in  $z_1, y_2, z_2, x_3, y_3, z_3$ . Hence, we can eliminate these six unknowns from (6.17) and (6.18). From (6.17), one obtains

$$\begin{aligned} z_1 &= t_{17}x_1 + t_{18}y_1 + t_{19}x_2 + t_{20}, \\ y_2 &= -(t_4x_1 + t_8y_1 + t_6x_2)/t_9, \\ x_3 &= -(s_1x_1 + s_2x_2)/s_3, \\ y_3 &= t_{11}x_1 + t_{12}y_1 + t_{13}x_2, \\ z_2 &= t_{21}x_1 + t_{22}y_1 + t_{23}x_2 + t_{24}, \end{aligned} \quad (6.19)$$

where  $t_i$  are constants for given tensions. Then, substituting (6.19) into (6.18), one gets

$$a_i x_1^2 + b_i y_1^2 + c_i x_2^2 + d_i x_1 y_1 + e_i y_1 x_2 + f_i x_2 x_1 + g_i x_1 + h_i y_1 + i_i x_2 + j_i = 0, \quad (6.20)$$

where  $a_i, b_i, \dots, j_i$  ( $i = 1, 2, 3$ ) are constants for given tensions.

The polynomial system given by (6.20) consists of 3 quadratic equations in  $x_1, y_1$  and  $x_2$ . The total degree of this polynomial system is 8. According to Bezout's theorem, this system has at most 8 isolated solutions in the complex space.

This section presents an analytic algorithm to address the general case of the above inverse kinematics problem. The proposed algorithm is based on Roth's Diallytic elimination approach [18]. The three equations given by (6.20) are actually the general expressions of three quadratic surfaces. To find the solutions of (6.20) is to find all common intersection points of three quadratic surfaces. In [18], Roth proposed a Diallytic elimination approach to eliminate two unknowns without increasing the power products and without increasing the degree of the system. The principle is based on the fact that the derivatives of the determinant of the Jacobian of a system of equations written in terms of homogeneous coordinates have the same zeros as the original system of equations. Here, Roth's approach is modified and used to solve (6.20) for the general case.

Suppose that  $x_2$  is suppressed, (6.20) can be written as

$$a_i x_1^2 + b_i y_1^2 + d_i x_1 y_1 + k_i x_1 + u_i y_1 + v_i = 0, \quad (6.21)$$

where  $k_i = f_i x_2 + g_i, u_i = e_i x_2 + h_i$  and  $v_i = c_i x_2^2 + i_i x_2 + j_i$  ( $i = 1, 2, 3$ ).

Now, there are three equations and six power products. Hence, at least three more equations are needed. Rewriting (6.21) into the form with homogeneous coordinates by substituting  $x_1 = X/T, y_1 = Y/T$  and then multiplying by  $T^2$ , one gets

$$a_i X^2 + b_i Y^2 + d_i XY + k_i XT + u_i YT + v_i T^2 = 0. \quad (6.22)$$

If the left-hand side of (6.22) is given by  $F_i$  ( $i = 1, 2, 3$ ), (6.22) can be re-written as

$$F_{iX}X + F_{iY}Y + F_{iT}T = 0, \quad (6.23)$$

where

$$\begin{aligned} F_{iX} &= \frac{\partial F_i}{\partial X} = 2a_iX + d_iY + k_iT, \\ F_{iY} &= \frac{\partial F_i}{\partial Y} = 2b_iY + d_iX + u_iT, \\ F_{iT} &= \frac{\partial F_i}{\partial T} = k_iX + u_iY + 2v_iT. \end{aligned} \quad (6.24)$$

Hence, (6.23) can be re-written in the following matrix form:

$$\mathbf{J}\mathbf{X}_1 = \mathbf{0}, \quad (6.25)$$

where  $\mathbf{X}_1 = [X, Y, T]^T$  and  $\mathbf{J}$  is the Jacobian matrix:

$$\mathbf{J} = \begin{bmatrix} F_{1X} & F_{1Y} & F_{1T} \\ F_{2X} & F_{2Y} & F_{2T} \\ F_{3X} & F_{3Y} & F_{3T} \end{bmatrix}. \quad (6.26)$$

In order to make  $\mathbf{X}_1$  to be not a zero vector, the determinant of the above Jacobian matrix must be zero:

$$|\mathbf{J}| = 0. \quad (6.27)$$

Thus,

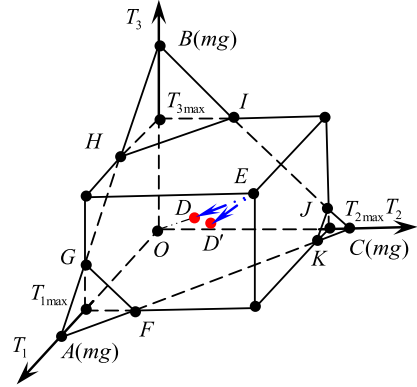
$$\begin{aligned} \frac{\partial |\mathbf{J}|}{\partial X} &= 3AX^2 + 2BXY + 2CXT + DY^2 + ET^2 + FYT = 0, \\ \frac{\partial |\mathbf{J}|}{\partial Y} &= BX^2 + 2DXY + FXT + 3GY^2 + 2HYT + IT^2 = 0, \\ \frac{\partial |\mathbf{J}|}{\partial T} &= CX^2 + 2EXT + FXY + HY^2 + 2IYT + 3JT^2 = 0, \end{aligned} \quad (6.28)$$

where  $A, B, \dots, K$  are functions of  $x_2$ . The six equations in (6.22) and (6.28) can be written in the following matrix form:

$$\mathbf{M}\mathbf{X}_2 = \mathbf{0}, \quad (6.29)$$

where  $\mathbf{X}_2 = [X^2, Y^2, XY, XT, YT, T^2]^T$ . In order to make  $\mathbf{X}_2$  to be not a zero vector, the determinant of matrix  $\mathbf{M}$  must be zero. This determinant is an eight-degree polynomial in  $x_2$ . The coefficients of this polynomial are functions of the coefficients of the original three equations. Hence,  $x_2$  can be easily solved with Matlab. For every real root  $x_2$  substituted into (6.29), a linear system in  $(x_1^2, y_1^2, x_1y_1, x_1, y_1)$  will be available by setting  $T$  to 1. Then, a solution of  $x_1$  and  $y_1$  can be obtained

**Fig. 6.9** Possible workspace of the tensions ( $mg$  is the weight of the payload)



by solving this linear system. When  $x_1, y_1$  and  $x_2$  are available, the other six unknowns ( $z_1, y_2, z_2, x_3, y_3, z_3$ ) can be calculated with (6.19). When  $x_i, y_i$  and  $z_i$  ( $i = 1, 2, 3$ ) are available, the position coordinates ( $x_{qi}, y_{qi}, z_{qi}, i = 1, 2, 3$ ) of the robots can be obtained. Theoretically speaking, there are up to eight common intersection points of three quadratic surfaces. The case studies conducted later show that usually only six or less real solutions can be found by (6.20) for the 3-D cable towing.

The above algorithm can solve the general inverse kinematics problem. Unfortunately, it fails in the special case with the attachment points lie in the horizontal plane which is discussed in greater detail in [9].

Referring to Fig. 6.9, in order to address the cooperation in the manipulation task, it is useful to define the so-called *tension ratio*. If the payload capacity of robot  $Q_i$  is  $T_{imax}$ , the tension ratio of cable  $i$  can be defined as

$$c_{ri} = T_i / T_{imax}. \tag{6.30}$$

If all robots were to share the load equally, normalized to their strengths, the tension ratios  $c_{ri}$  ( $i = 1, 2, 3$ ) should be the same. Otherwise, the robots are not, strictly speaking, cooperating in a fair way. In the case with three robots, we want  $c_{r1} = c_{r2} = c_{r3} = c_r$ , which corresponds to the line  $\overline{EO}$  inside the rectangular cuboid in Fig. 6.9.  $E$  represents the point with the maximal tension ratio  $c_r = 1$ . At this point, the tension of every cable reaches the payload capacity of every robot. In this condition of maximal cooperation, the tensions can be directly obtained from the tension ratio  $c_r$ .

For the 3-D cooperative towing with three aerial robots, the body-fixed frame can be chosen by taking  $P_1$  as the origin  $\tilde{O}$ ,  $P_1 P_2$  as the  $\tilde{x}$  axis and triangle  $P_1 P_2 P_3$  as the  $\tilde{O}\tilde{x}\tilde{y}$  plane.

Suppose that the attachment points ( $P_1, P_2, P_3$ ) of the payload form an arbitrary triangle. Their coordinates in the body-fixed frame are given by  $\tilde{\mathbf{p}}_1 = [0, 0, 0]^T m$ ,  $\tilde{\mathbf{p}}_2 = [1, 0, 0]^T m$  and  $\tilde{\mathbf{p}}_3 = [0.8, 0.7, 0]^T m$ . The center of mass does not lie in the plane of triangle  $P_1 P_2 P_3$ . Instead, its position in the body-fixed frame is given by  $\tilde{\mathbf{r}} = [0.7, 0.2, -0.3]^T m$ . The lengths of three cables are  $l_1 = l_2 = l_3 = 1.5$  m. The

**Table 6.3** Solutions for a general payload with  $c_r = 0.9$ ,  $\phi = 25^\circ$ ,  $\theta = 15^\circ$  and  $\psi = -5^\circ$ 

No.	1	2	3	4	5	6
$x_{q1}(m)$	-0.024	-0.590	1.783	1.469	-0.111	-0.456
$y_{q1}(m)$	1.473	-0.319	0.527	1.294	1.428	1.159
$z_{q1}(m)$	2.621	1.845	1.738	2.196	2.618	2.560
$x_{q2}(m)$	2.385	0.650	0.030	1.039	2.548	2.489
$y_{q2}(m)$	1.453	1.464	0.085	1.656	-0.166	-0.244
$z_{q2}(m)$	1.790	2.186	1.630	2.195	0.937	0.911
$x_{q3}(m)$	0.588	2.531	1.293	0.646	0.510	0.821
$y_{q3}(m)$	0.071	1.405	1.977	0.028	1.522	1.791
$z_{q3}(m)$	1.979	2.214	2.781	1.944	2.728	2.794

weight of the payload is  $mg = 100$  N. The payload capacities of three robots are respectively  $T_{1max} = 60$  N,  $T_{2max} = 70$  N and  $T_{3max} = 80$  N. In this very general case, if the position of the payload is chosen as  $\mathbf{r} = [1, 1, 1]^T m$  and the tension ratios are chosen as the same with  $c_r = 0.9$  and the desired orientation is given by ( $\phi = 25^\circ$ ,  $\theta = 15^\circ$ ,  $\psi = -5^\circ$ ), six solutions for the inverse kinematics problem can be found and listed in Table 6.3, which corresponds to the four configurations as shown in Fig. 6.10.

Six sequences of configurations can be obtained by reducing  $c_r$  from 1 along line  $EO$  in Fig. 6.9. These sequences are shown in Fig. 6.11 in which sequences 1 and 2 correspond to a range of  $c_r \in [0.532, 1]$ , sequences 3 and 4 correspond to a range of  $c_r \in [0.575, 1]$ , and sequences 5 to 6 correspond to a range of  $c_r \in [0.9, 1]$ . In other words, when the tension ratio  $c_r$  is less than 0.9 and greater than 0.575, the inverse kinematics problem has only four solutions. When the tension ratio  $c_r$  is less than 0.575, the inverse kinematics problem has only two solutions. In this general case, the minimal tension ratio  $c_r = 0.532$  can also be obtained numerically using a line search. Obviously, in the general case, the minimal tension ratio 0.532 is greater than 0.472 calculated with  $c_r \sum_{i=1}^3 T_{imax} = mg$ . Also, when  $c_r$  reaches its minimal valid value 0.532, the three cables do not lie in vertical positions, see the dashed lines in Figs. 6.11(a) and (b).

## 6.5 The Set of Valid Tensions

For a given set of tensions, we can find several equilibrium configurations. However, the tensions cannot be chosen arbitrarily. The tension of every cable should be in a range from a positive lower threshold to the payload capacity  $T_{imax}$  of the robot, i.e.,  $T_i \in [0, T_{imax}]$ . In the case with three robots, it would seem that any point in the rectangular cuboid with side length  $T_{imax}$  ( $i = 1, 2, 3$ ) as shown in Fig. 6.9 is a valid choice of tensions. However, this is not true. First, the tensions of three cables

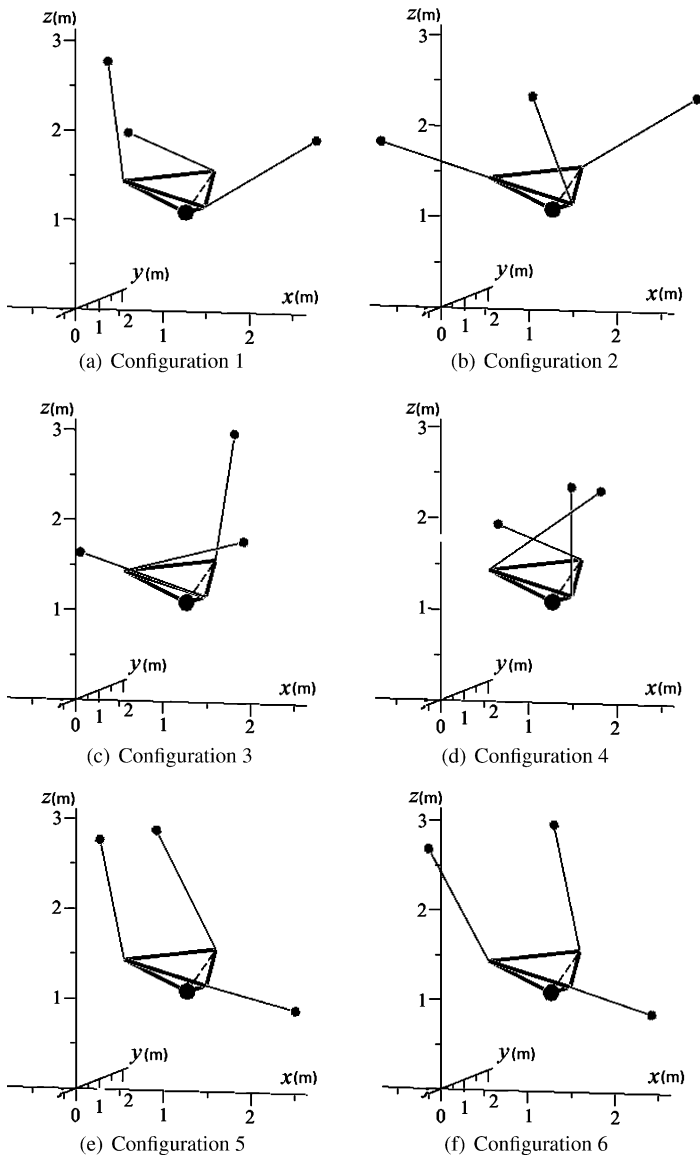


**Fig. 6.10** Configurations for a general payload in a general configuration ( $\mathbf{r} = [1, 1, 1]^T m$ ,  $\phi = 25^\circ$ ,  $\theta = 15^\circ$  and  $\psi = -5^\circ$ ), with  $c_r = 0.9$

should satisfy the following condition:

$$\sum_{i=1}^3 T_i \geq mg. \tag{6.31}$$

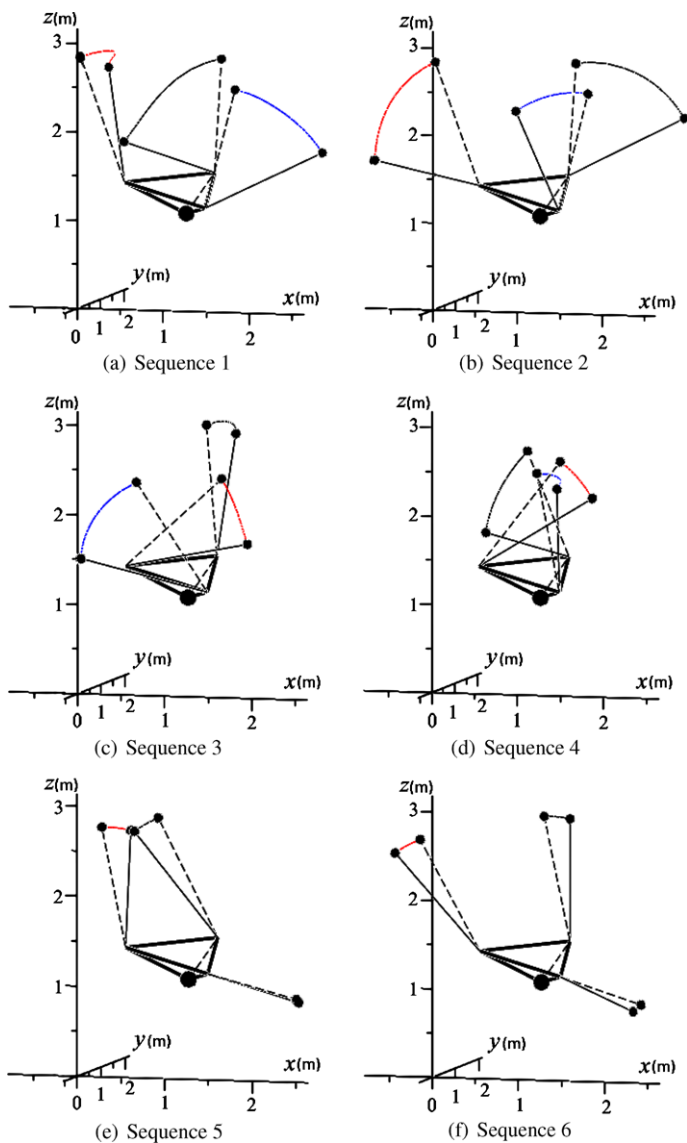


**Fig. 6.11** Sequences of configurations for a general configuration ( $\mathbf{r} = [1, 1, 1]^T m$ ,  $\phi = 25^\circ$ ,  $\theta = 15^\circ$  and  $\psi = -5^\circ$ ), with different tension ratios

This condition shows that the possible work point for the tensions should be in the region above the plane  $ABC$  with  $\sum_{i=1}^3 T_i = mg$ . However, even in this region, not every point represents a valid set of tensions. For instance, in general, points on the boundary  $FGHIJKF$  are not realistic if a desired orientation is specified.

Accordingly, we determine the *tension workspace*, the set of valid tensions. First, the vertex  $E$  in Fig. 6.9 should be a valid point. Otherwise, the tension workspace



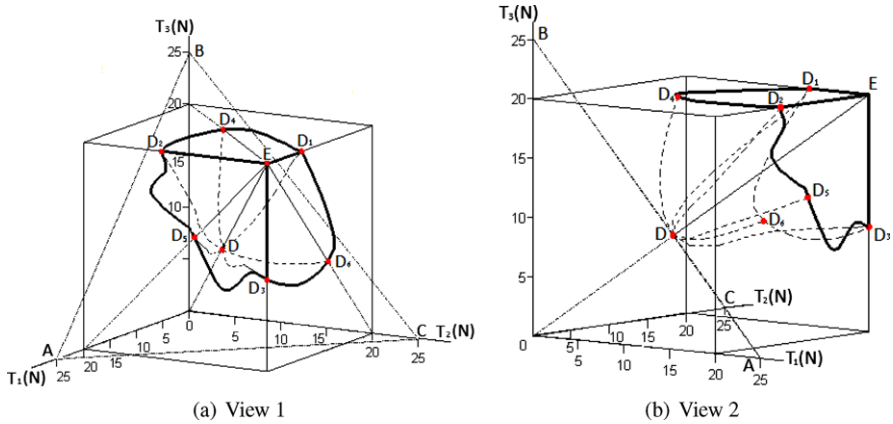


**Fig. 6.12** Tension workspace for an equilateral triangle payload with  $\phi = 25^\circ$ ,  $\theta = 15^\circ$ ,  $\psi = -5^\circ$

is the null set. Second, the tension workspace should lie in the half plane above the plane  $ABC$  defined  $\sum_{i=1}^3 T_i = mg$ . Hence, it should be closed by three planes, each perpendicular to one of the axes, and a surface that lies above  $ABC$  as shown in Fig. 6.12. To compute the boundary of this workspace, we start from  $c_r = 1$  (which corresponds to point  $E$  in Fig. 6.9) and gradually decrease  $c_r$  with a small step size,  $\Delta c_r$ , along different rays in the workspace numerically. See Fig. 6.12. More details are available in [9].

### 6.6 Stability Analysis

The equilibrium configurations have been obtained from the case studies in both direct and inverse kinematics analysis. However, we have not discussed the stability of the equilibrium points. Clearly the payload will not stay in configurations that are unstable. Thus it is necessary to able to find solutions that are stable.

The obvious approach to analyze the stability is to derive the Hessian matrix of the system. If all eigenvalues  $\lambda_i$  ( $i = 1, 2, \dots, n$ ) of the Hessian matrix are strictly positive, the corresponding equilibrium configuration can be regarded as stable. Otherwise, the configuration is either unstable (one of the eigenvalues is strictly negative) or requires higher order analysis (all eigenvalues are non negative).

The position and orientation of the payload can be defined by the position  $\mathbf{r} = [x, y, z]^T$  of its center of mass and the rotation matrix  $\mathbf{R}$  in which there are three orientation angles  $(\phi, \theta, \psi)$ . Hence, six variable  $(x, y, z, \phi, \theta, \psi)$  can be used to define the position and orientation of the payload.

#### 6.6.1 Case with Two Cables

In the equilibrium configurations as shown in Figs. 6.6(b), (c) and (d), the payload is suspended by only two cables. Considering the geometric constraints imposed by

the two cables, the payload has four degrees of freedom. Hence, only four of the six variables  $(x, y, z, \phi, \theta, \psi)$  are independent. Referring to the geometric constraints given by (6.4), the coordinate  $x$  can be eliminated and  $z$  can be expressed as the function of  $(y, \phi, \theta, \psi)$ , which are used as four independent variables. The potential energy of the payload can be given by

$$V = mgz = mgz(y, \phi, \theta, \psi). \quad (6.32)$$

Hence, the Hessian matrix can be given as

$$\mathbf{H} = mg \begin{bmatrix} \frac{\partial^2 z}{\partial y^2} & \frac{\partial^2 z}{\partial y \partial \phi} & \frac{\partial^2 z}{\partial y \partial \theta} & \frac{\partial^2 z}{\partial y \partial \psi} \\ \frac{\partial^2 z}{\partial \phi \partial y} & \frac{\partial^2 z}{\partial \phi^2} & \frac{\partial^2 z}{\partial \phi \partial \theta} & \frac{\partial^2 z}{\partial \phi \partial \psi} \\ \frac{\partial^2 z}{\partial \theta \partial y} & \frac{\partial^2 z}{\partial \theta \partial \phi} & \frac{\partial^2 z}{\partial \theta^2} & \frac{\partial^2 z}{\partial \theta \partial \psi} \\ \frac{\partial^2 z}{\partial \psi \partial y} & \frac{\partial^2 z}{\partial \psi \partial \phi} & \frac{\partial^2 z}{\partial \psi \partial \theta} & \frac{\partial^2 z}{\partial \psi^2} \end{bmatrix}. \quad (6.33)$$

Now, the focus is how to obtain the above Hessian matrix. From (6.4), one gets

$$\begin{aligned} (x + u_{11})^2 + (y + u_{12})^2 + (z + u_{13})^2 &= l_1^2, \\ (x + u_{21})^2 + (y + u_{22})^2 + (z + u_{23})^2 &= l_2^2, \end{aligned} \quad (6.34)$$

where

$$\begin{aligned} u_{11} &= r_{11}(\tilde{x}_{p1} - \tilde{x}) + r_{12}(\tilde{y}_{p1} - \tilde{y}) + r_{13}(\tilde{z}_{p1} - \tilde{z}) - x_{q1}, \\ u_{12} &= r_{21}(\tilde{x}_{p1} - \tilde{x}) + r_{22}(\tilde{y}_{p1} - \tilde{y}) + r_{23}(\tilde{z}_{p1} - \tilde{z}) - y_{q1}, \\ u_{13} &= r_{31}(\tilde{x}_{p1} - \tilde{x}) + r_{32}(\tilde{y}_{p1} - \tilde{y}) + r_{33}(\tilde{z}_{p1} - \tilde{z}) - z_{q1}, \\ u_{21} &= r_{11}(\tilde{x}_{p2} - \tilde{x}) + r_{12}(\tilde{y}_{p2} - \tilde{y}) + r_{13}(\tilde{z}_{p2} - \tilde{z}) - x_{q2}, \\ u_{22} &= r_{21}(\tilde{x}_{p2} - \tilde{x}) + r_{22}(\tilde{y}_{p2} - \tilde{y}) + r_{23}(\tilde{z}_{p2} - \tilde{z}) - y_{q2}, \\ u_{23} &= r_{31}(\tilde{x}_{p2} - \tilde{x}) + r_{32}(\tilde{y}_{p2} - \tilde{y}) + r_{33}(\tilde{z}_{p2} - \tilde{z}) - z_{q2}, \end{aligned} \quad (6.35)$$

and  $r_{ij}$  ( $i, j = 1, 2, 3$ ) are the entries of the rotation matrix  $\mathbf{R}$  and given as follows:

$$\begin{aligned} r_{11} &= \cos \theta \cos \psi, \\ r_{12} &= \sin \phi \sin \theta \cos \psi - \cos \phi \sin \psi, \\ r_{13} &= \cos \phi \sin \theta \cos \psi + \sin \phi \sin \psi, \\ r_{21} &= \cos \theta \sin \psi, \\ r_{22} &= \sin \phi \sin \theta \sin \psi + \cos \phi \cos \psi, \\ r_{23} &= \cos \phi \sin \theta \sin \psi - \sin \phi \cos \psi, \\ r_{31} &= -\sin \theta, \end{aligned} \quad (6.36)$$

$$\begin{aligned} r_{32} &= \sin \phi \cos \theta, \\ r_{33} &= \cos \phi \cos \theta. \end{aligned}$$

Subtracting the first equation of (6.34) from the second equation of (6.34), one gets

$$2(u_{21} - u_{11})x + 2(u_{22} - u_{12})y + 2(u_{23} - u_{13})z = U_2 - U_1, \quad (6.37)$$

where

$$\begin{aligned} U_1 &= l_1^2 - u_{11}^2 - u_{12}^2 - u_{13}^2, \\ U_2 &= l_2^2 - u_{21}^2 - u_{22}^2 - u_{23}^2. \end{aligned} \quad (6.38)$$

From (6.37), one gets

$$\begin{aligned} x &= [(l_2^2 - u_{21}^2 - u_{22}^2 - u_{23}^2 - l_1^2 + u_{11}^2 + u_{12}^2 + u_{13}^2)/2 \\ &\quad - (u_{22} - u_{12})y - (u_{23} - u_{13})z]/(u_{21} - u_{11}). \end{aligned} \quad (6.39)$$

Substituting (6.39) into the first equation of (6.34), one gets

$$F = F(y, z, u_{11}, \dots, u_{23}) = F(y, z, \phi, \theta, \psi). \quad (6.40)$$

So,

$$\begin{aligned} \frac{\partial z}{\partial y} &= -F_y/F_z, & \frac{\partial z}{\partial \phi} &= -F_\phi/F_z, \\ \frac{\partial z}{\partial \theta} &= -F_\theta/F_z, & \frac{\partial z}{\partial \psi} &= -F_\psi/F_z. \end{aligned} \quad (6.41)$$

Therefore,

$$\begin{aligned} \frac{\partial^2 z}{\partial y^2} &= -\frac{F_{yy}F_z - F_yF_{zy}}{F_z^2}, & \frac{\partial^2 z}{\partial y \partial \phi} &= -\frac{F_{y\phi}F_z - F_yF_{z\phi}}{F_z^2}, \\ \frac{\partial^2 z}{\partial y \partial \theta} &= -\frac{F_{y\theta}F_z - F_yF_{z\theta}}{F_z^2}, & \frac{\partial^2 z}{\partial y \partial \psi} &= -\frac{F_{y\psi}F_z - F_yF_{z\psi}}{F_z^2}, \\ \frac{\partial^2 z}{\partial \phi \partial y} &= -\frac{F_{\phi y}F_z - F_\phi F_{zy}}{F_z^2}, & \frac{\partial^2 z}{\partial \phi^2} &= -\frac{F_{\phi\phi}F_z - F_\phi F_{z\phi}}{F_z^2}, \\ \frac{\partial^2 z}{\partial \phi \partial \theta} &= -\frac{F_{\phi\theta}F_z - F_\phi F_{z\theta}}{F_z^2}, & \frac{\partial^2 z}{\partial \phi \partial \psi} &= -\frac{F_{\phi\psi}F_z - F_\phi F_{z\psi}}{F_z^2}, \\ \frac{\partial^2 z}{\partial \theta \partial y} &= -\frac{F_{\theta y}F_z - F_\theta F_{zy}}{F_z^2}, & \frac{\partial^2 z}{\partial \theta \partial \phi} &= -\frac{F_{\theta\phi}F_z - F_\theta F_{z\phi}}{F_z^2}, \\ \frac{\partial^2 z}{\partial \theta^2} &= -\frac{F_{\theta\theta}F_z - F_\theta F_{z\theta}}{F_z^2}, & \frac{\partial^2 z}{\partial \theta \partial \psi} &= -\frac{F_{\theta\psi}F_z - F_\theta F_{z\psi}}{F_z^2}, \end{aligned} \quad (6.42)$$

**Table 6.4** Eigenvalues of the Hessian matrices of the equilibrium configurations with two cables

Configuration	Fig. 6.6(a)	Fig. 6.6(b)	Fig. 6.6(c)	Fig. 6.6(d)
$\lambda_1$	1.635	0.092	0.091	0.091
$\lambda_2$	0.344	+0.000	0.000	9.214
$\lambda_3$	0.086	9.039	-0.150	-0.150
$\lambda_4$	+0.000	-0.367	-0.153	-0.153

$$\frac{\partial^2 z}{\partial \psi \partial y} = -\frac{F_{\psi y} F_z - F_{\psi} F_{zy}}{F_z^2}, \quad \frac{\partial^2 z}{\partial \psi \partial \phi} = -\frac{F_{\psi \phi} F_z - F_{\psi} F_{z\phi}}{F_z^2},$$

$$\frac{\partial^2 z}{\partial \psi \partial \theta} = -\frac{F_{\psi \theta} F_z - F_{\psi} F_{z\theta}}{F_z^2}, \quad \frac{\partial^2 z}{\partial \psi^2} = -\frac{F_{\psi \psi} F_z - F_{\psi} F_{z\psi}}{F_z^2}.$$

If  $F$  is directly expressed as the function of  $(y, z, \phi, \theta, \psi)$ , the expression of  $F$  is so complicated that standard symbolic manipulation packages cannot handle the derivation. Hence, all derivatives ( $F_y, F_z, F_\phi, F_\theta, F_\psi, F_{zy}, F_{z\phi}, F_{z\theta}, F_{z\psi}, F_{yy}, F_{y\phi}, F_{y\theta}, F_{y\psi}, F_{\phi y}, F_{\phi\phi}, F_{\phi\theta}, F_{\phi\psi}, F_{\theta y}, F_{\theta\phi}, F_{\theta\theta}, F_{\theta\psi}, F_{\psi y}, F_{\psi\phi}, F_{\psi\theta}, F_{\psi\psi}$ ) of  $F$  with respect to  $(y, z, \phi, \theta, \psi)$  have to be computed individually and pieced together using the chain rule. Even so, the expressions of some second order derivatives are still very complicated. Substituting (6.42) into (6.33), the Hessian matrix is obtained and the eigenvalues of the Hessian matrix are determined.

Now the above developed approach is used to analyze the stability of the equilibrium configurations as shown in Fig. 6.6. Although the configuration of the payload as shown Fig. 6.6(a) coincides with its initial configuration as shown in Fig. 6.5, this configuration is obtained by supposing that the payload is suspended with two cables. Hence, the stability analysis of this configuration can be conducted by supposing that the payloads is suspended with only two relevant cables. If this configuration under this condition is stable, its corresponding initial configuration should be more stable.

For every equilibrium configuration as shown in Fig. 6.6, the positions of two relevant robots and two relevant attachment points and the center of mass as well as the orientation angles of the payload are know. Substituting all these parameters into (6.42) and then into (6.33), a Hessian matrix is available. The eigenvalues of the Hessian matrix can be easily evaluated by the package Matlab.

Table 6.4 lists the eigenvalues of the Hessian matrices of these equilibrium configurations. From this table, it can be seen that the configurations as shown in Fig. 6.6(a) are stable. But other configurations are unstable.

## 6.6.2 Case with Three Cables

In the equilibrium configurations as shown in Fig. 6.10, the payload is suspended by three cables. Considering the geometric constraints imposed by the three ca-

bles, the payload has three degrees of freedom. Hence, three of the six variables  $(x, y, z, \phi, \theta, \psi)$  are independent.

Referring to the geometric constraints given by (6.4), the coordinates  $(x, y)$  can be eliminated and  $z$  can be expressed as the function of the orientation angles  $(\phi, \theta, \psi)$ , which are used as three independent variables. The potential energy of the payload can be given by

$$V = mgz = mgz(\phi, \theta, \psi). \quad (6.43)$$

Hence, the Hessian matrix can be given as

$$\mathbf{H} = mg \begin{bmatrix} \frac{\partial^2 z}{\partial \phi^2} & \frac{\partial^2 z}{\partial \phi \partial \theta} & \frac{\partial^2 z}{\partial \phi \partial \psi} \\ \frac{\partial^2 z}{\partial \theta \partial \phi} & \frac{\partial^2 z}{\partial \theta^2} & \frac{\partial^2 z}{\partial \theta \partial \psi} \\ \frac{\partial^2 z}{\partial \psi \partial \phi} & \frac{\partial^2 z}{\partial \psi \partial \theta} & \frac{\partial^2 z}{\partial \psi^2} \end{bmatrix}. \quad (6.44)$$

Now, the focus is how to obtain the above Hessian matrix. From (6.4), one gets

$$\begin{aligned} (x + u_{11})^2 + (y + u_{12})^2 + (z + u_{13})^2 &= l_1^2, \\ (x + u_{21})^2 + (y + u_{22})^2 + (z + u_{23})^2 &= l_2^2, \\ (x + u_{31})^2 + (y + u_{32})^2 + (z + u_{33})^2 &= l_3^2, \end{aligned} \quad (6.45)$$

where

$$\begin{aligned} u_{11} &= r_{11}(\tilde{x}_{p1} - \tilde{x}) + r_{12}(\tilde{y}_{p1} - \tilde{y}) + r_{13}(\tilde{z}_{p1} - \tilde{z}) - x_{q1}, \\ u_{12} &= r_{21}(\tilde{x}_{p1} - \tilde{x}) + r_{22}(\tilde{y}_{p1} - \tilde{y}) + r_{23}(\tilde{z}_{p1} - \tilde{z}) - y_{q1}, \\ u_{13} &= r_{31}(\tilde{x}_{p1} - \tilde{x}) + r_{32}(\tilde{y}_{p1} - \tilde{y}) + r_{33}(\tilde{z}_{p1} - \tilde{z}) - z_{q1}, \\ u_{21} &= r_{11}(\tilde{x}_{p2} - \tilde{x}) + r_{12}(\tilde{y}_{p2} - \tilde{y}) + r_{13}(\tilde{z}_{p2} - \tilde{z}) - x_{q2}, \\ u_{22} &= r_{21}(\tilde{x}_{p2} - \tilde{x}) + r_{22}(\tilde{y}_{p2} - \tilde{y}) + r_{23}(\tilde{z}_{p2} - \tilde{z}) - y_{q2}, \\ u_{23} &= r_{31}(\tilde{x}_{p2} - \tilde{x}) + r_{32}(\tilde{y}_{p2} - \tilde{y}) + r_{33}(\tilde{z}_{p2} - \tilde{z}) - z_{q2}, \\ u_{31} &= r_{11}(\tilde{x}_{p3} - \tilde{x}) + r_{12}(\tilde{y}_{p3} - \tilde{y}) + r_{13}(\tilde{z}_{p3} - \tilde{z}) - x_{q3}, \\ u_{32} &= r_{21}(\tilde{x}_{p3} - \tilde{x}) + r_{22}(\tilde{y}_{p3} - \tilde{y}) + r_{23}(\tilde{z}_{p3} - \tilde{z}) - y_{q3}, \\ u_{33} &= r_{31}(\tilde{x}_{p3} - \tilde{x}) + r_{32}(\tilde{y}_{p3} - \tilde{y}) + r_{33}(\tilde{z}_{p3} - \tilde{z}) - z_{q3}, \end{aligned} \quad (6.46)$$

and  $r_{ij}$  ( $i, j = 1, 2, 3$ ) are the entries of the rotation matrix  $\mathbf{R}$  and given by (6.36). Respectively subtracting the first equation of (6.45) from the second and the third equations of (6.45), one gets

$$\begin{aligned} 2(u_{21} - u_{11})x + 2(u_{22} - u_{12})y + 2(u_{23} - u_{13})z &= U_2 - U_1, \\ 2(u_{31} - u_{11})x + 2(u_{32} - u_{12})y + 2(u_{33} - u_{13})z &= U_3 - U_1, \end{aligned} \quad (6.47)$$

where

$$\begin{aligned} U_1 &= l_1^2 - u_{11}^2 - u_{12}^2 - u_{13}^2, \\ U_2 &= l_2^2 - u_{21}^2 - u_{22}^2 - u_{23}^2, \\ U_3 &= l_3^2 - u_{31}^2 - u_{32}^2 - u_{33}^2. \end{aligned} \tag{6.48}$$

From (6.47), one gets

$$\begin{aligned} x &= \frac{-u_{32}u_{23} + u_{32}u_{13} + u_{12}u_{23} + u_{22}u_{33} - u_{22}u_{13} - u_{12}u_{33}}{u_{21}u_{32} - u_{21}u_{12} - u_{11}u_{32} - u_{22}u_{31} + u_{22}u_{11} + u_{12}u_{31}} z \\ &\quad + \frac{u_{32}U_2 - u_{32}U_1 - u_{12}U_2 - u_{22}U_3 + u_{22}U_1 + u_{12}U_3}{2(u_{21}u_{32} - u_{21}u_{12} - u_{11}u_{32} - u_{22}u_{31} + u_{22}u_{11} + u_{12}u_{31})}, \\ y &= \frac{u_{31}u_{23} - u_{31}u_{13} - u_{11}u_{23} - u_{21}u_{33} + u_{21}u_{13} + u_{11}u_{33}}{u_{21}u_{32} - u_{21}u_{12} - u_{11}u_{32} - u_{22}u_{31} + u_{22}u_{11} + u_{12}u_{31}} z \\ &\quad - \frac{u_{31}U_2 - u_{31}U_1 - u_{11}U_2 - u_{21}U_3 + u_{21}U_1 + u_{11}U_3}{2(u_{21}u_{32} - u_{21}u_{12} - u_{11}u_{32} - u_{22}u_{31} + u_{22}u_{11} + u_{12}u_{31})}. \end{aligned} \tag{6.49}$$

Substituting (6.49) into the first equation of (6.45), one gets

$$F(z, u_{11}, \dots, u_{33}) = F(z, \phi, \theta, \psi) = 0. \tag{6.50}$$

So,

$$\frac{\partial z}{\partial \phi} = -F_\phi / F_z, \quad \frac{\partial z}{\partial \theta} = -F_\theta / F_z, \quad \frac{\partial z}{\partial \psi} = -F_\psi / F_z. \tag{6.51}$$

Hence,

$$\begin{aligned} \frac{\partial^2 z}{\partial \phi^2} &= -\frac{F_{\phi\phi}F_z - F_\phi F_{z\phi}}{F_z^2}, \\ \frac{\partial^2 z}{\partial \phi \partial \theta} &= -\frac{F_{\phi\theta}F_z - F_\phi F_{z\theta}}{F_z^2}, \\ \frac{\partial^2 z}{\partial \phi \partial \psi} &= -\frac{F_{\phi\psi}F_z - F_\phi F_{z\psi}}{F_z^2}, \\ \frac{\partial^2 z}{\partial \theta \partial \phi} &= -\frac{F_{\theta\phi}F_z - F_\theta F_{z\phi}}{F_z^2}, \\ \frac{\partial^2 z}{\partial \theta^2} &= -\frac{F_{\theta\theta}F_z - F_\theta F_{z\theta}}{F_z^2}, \end{aligned} \tag{6.52}$$

**Table 6.5** Eigenvalues of Hessian matrices of the equilibrium configurations in Fig. 6.10

No.	1	2	3	4	5	6
$\lambda_1$	2.789	1.345	1.101	0.625	11.001	29.549
$\lambda_2$	0.495	0.729	0.428	0.080	0.823	0.844
$\lambda_3$	0.009	0.196	0.043	-0.350	0.450	0.689

$$\frac{\partial^2 z}{\partial \theta \partial \psi} = -\frac{F_{\theta \psi} F_z - F_{\theta} F_{z \psi}}{F_z^2},$$

$$\frac{\partial^2 z}{\partial \psi \partial \phi} = -\frac{F_{\psi \phi} F_z - F_{\psi} F_{z \phi}}{F_z^2},$$

$$\frac{\partial^2 z}{\partial \psi \partial \theta} = -\frac{F_{\psi \theta} F_z - F_{\psi} F_{z \theta}}{F_z^2},$$

$$\frac{\partial^2 z}{\partial \psi^2} = -\frac{F_{\psi \psi} F_z - F_{\psi} F_{z \psi}}{F_z^2}.$$

Equation (6.50) shows that  $F$  is a function of  $(z, \phi, \theta, \psi)$ . Its derivatives with respect to  $(z, \phi, \theta, \psi)$  can be derived using the chain rule. Substituting (6.52) into (6.44), we can obtain a Hessian matrix which can be used to analyze the stability of the equilibrium configurations. For every equilibrium configuration, the positions of three relevant robots and three relevant attachment points and the center of mass as well as the orientation angles of the payload are known. Substituting all these parameters into (6.52) and then into (6.44), a Hessian matrix is available. The eigenvalues of the Hessian matrix can be easily evaluated by the package Matlab.

Table 6.5 lists the eigenvalues of the Hessian matrices of the six equilibrium configurations as shown in Fig. 6.10. From this table, it can be seen that configurations 1, 2, 3, 5 and 6 are stable. Only configuration 4 is unstable.

### 6.6.3 Case with Four Cables

In the equilibrium configurations as shown in Figs. 6.7(b), (c) and (d), the payload is suspended by four cables. Considering the geometric constraints imposed by the four cables, the payload has two degrees of freedom. Hence, only two of the six variables  $(x, y, z, \phi, \theta, \psi)$  are independent. If  $(\theta, \psi)$  are used as the two independent variables, the Hessian matrix can be given by

$$\mathbf{H} = mg \begin{bmatrix} \frac{\partial^2 z}{\partial \theta^2} & \frac{\partial^2 z}{\partial \theta \partial \psi} \\ \frac{\partial^2 z}{\partial \psi \partial \theta} & \frac{\partial^2 z}{\partial \psi^2} \end{bmatrix}. \quad (6.53)$$

Now, the focus is how to obtain the above Hessian matrix. From (6.4), one gets

$$\begin{aligned}
 (x + u_{11})^2 + (y + u_{12})^2 + (z + u_{13})^2 &= l_1^2, \\
 (x + u_{21})^2 + (y + u_{22})^2 + (z + u_{23})^2 &= l_2^2, \\
 (x + u_{31})^2 + (y + u_{32})^2 + (z + u_{33})^2 &= l_3^2, \\
 (x + u_{41})^2 + (y + u_{42})^2 + (z + u_{43})^2 &= l_4^2,
 \end{aligned} \tag{6.54}$$

where

$$\begin{aligned}
 u_{11} &= r_{11}(\tilde{x}_{p1} - \tilde{x}) + r_{12}(\tilde{y}_{p1} - \tilde{y}) + r_{13}(\tilde{z}_{p1} - \tilde{z}) - x_{q1}, \\
 u_{12} &= r_{21}(\tilde{x}_{p1} - \tilde{x}) + r_{22}(\tilde{y}_{p1} - \tilde{y}) + r_{23}(\tilde{z}_{p1} - \tilde{z}) - y_{q1}, \\
 u_{13} &= r_{31}(\tilde{x}_{p1} - \tilde{x}) + r_{32}(\tilde{y}_{p1} - \tilde{y}) + r_{33}(\tilde{z}_{p1} - \tilde{z}) - z_{q1}, \\
 u_{21} &= r_{11}(\tilde{x}_{p2} - \tilde{x}) + r_{12}(\tilde{y}_{p2} - \tilde{y}) + r_{13}(\tilde{z}_{p2} - \tilde{z}) - x_{q2}, \\
 u_{22} &= r_{21}(\tilde{x}_{p2} - \tilde{x}) + r_{22}(\tilde{y}_{p2} - \tilde{y}) + r_{23}(\tilde{z}_{p2} - \tilde{z}) - y_{q2}, \\
 u_{23} &= r_{31}(\tilde{x}_{p2} - \tilde{x}) + r_{32}(\tilde{y}_{p2} - \tilde{y}) + r_{33}(\tilde{z}_{p2} - \tilde{z}) - z_{q2}, \\
 u_{31} &= r_{11}(\tilde{x}_{p3} - \tilde{x}) + r_{12}(\tilde{y}_{p3} - \tilde{y}) + r_{13}(\tilde{z}_{p3} - \tilde{z}) - x_{q3}, \\
 u_{32} &= r_{21}(\tilde{x}_{p3} - \tilde{x}) + r_{22}(\tilde{y}_{p3} - \tilde{y}) + r_{23}(\tilde{z}_{p3} - \tilde{z}) - y_{q3}, \\
 u_{33} &= r_{31}(\tilde{x}_{p3} - \tilde{x}) + r_{32}(\tilde{y}_{p3} - \tilde{y}) + r_{33}(\tilde{z}_{p3} - \tilde{z}) - z_{q3}, \\
 u_{41} &= r_{11}(\tilde{x}_{p4} - \tilde{x}) + r_{12}(\tilde{y}_{p4} - \tilde{y}) + r_{13}(\tilde{z}_{p4} - \tilde{z}) - x_{q4}, \\
 u_{42} &= r_{21}(\tilde{x}_{p4} - \tilde{x}) + r_{22}(\tilde{y}_{p4} - \tilde{y}) + r_{23}(\tilde{z}_{p4} - \tilde{z}) - y_{q4}, \\
 u_{43} &= r_{31}(\tilde{x}_{p4} - \tilde{x}) + r_{32}(\tilde{y}_{p4} - \tilde{y}) + r_{33}(\tilde{z}_{p4} - \tilde{z}) - z_{q4},
 \end{aligned} \tag{6.55}$$

and  $r_{ij}$  ( $i, j = 1, 2, 3$ ) are the entries of the rotation matrix  $\mathbf{R}$  and given by (6.36). From (6.54), one gets

$$\begin{aligned}
 x^2 + 2u_{11}x + y^2 + 2u_{12}y + z^2 + 2u_{13}z &= U_1, \\
 x^2 + 2u_{21}x + y^2 + 2u_{22}y + z^2 + 2u_{23}z &= U_2, \\
 x^2 + 2u_{31}x + y^2 + 2u_{32}y + z^2 + 2u_{33}z &= U_3, \\
 x^2 + 2u_{41}x + y^2 + 2u_{42}y + z^2 + 2u_{43}z &= U_4,
 \end{aligned} \tag{6.56}$$

where

$$\begin{aligned}
 U_1 &= l_1^2 - u_{11}^2 - u_{12}^2 - u_{13}^2, \\
 U_2 &= l_2^2 - u_{21}^2 - u_{22}^2 - u_{23}^2, \\
 U_3 &= l_3^2 - u_{31}^2 - u_{32}^2 - u_{33}^2, \\
 U_4 &= l_4^2 - u_{41}^2 - u_{42}^2 - u_{43}^2.
 \end{aligned} \tag{6.57}$$



From the first three equations of (6.56), one gets

$$\begin{aligned} 2(u_{21} - u_{11})x + 2(u_{22} - u_{12})y + 2(u_{23} - u_{13})z &= U_2 - U_1, \\ 2(u_{31} - u_{11})x + 2(u_{32} - u_{12})y + 2(u_{33} - u_{13})z &= U_3 - U_1. \end{aligned} \quad (6.58)$$

Hence,

$$\begin{aligned} x &= \frac{-u_{32}u_{23} + u_{32}u_{13} + u_{12}u_{23} + u_{22}u_{33} - u_{22}u_{13} - u_{12}u_{33}}{u_{21}u_{32} - u_{21}u_{12} - u_{11}u_{32} - u_{22}u_{31} + u_{22}u_{11} + u_{12}u_{31}}z \\ &\quad + \frac{u_{32}U_2 - u_{32}U_1 - u_{12}U_2 - u_{22}U_3 + u_{22}U_1 + u_{12}U_3}{2(u_{21}u_{32} - u_{21}u_{12} - u_{11}u_{32} - u_{22}u_{31} + u_{22}u_{11} + u_{12}u_{31})}, \\ y &= \frac{u_{31}u_{23} - u_{31}u_{13} - u_{11}u_{23} - u_{21}u_{33} + u_{21}u_{13} + u_{11}u_{33}}{u_{21}u_{32} - u_{21}u_{12} - u_{11}u_{32} - u_{22}u_{31} + u_{22}u_{11} + u_{12}u_{31}}z \\ &\quad - \frac{u_{31}U_2 - u_{31}U_1 - u_{11}U_2 - u_{21}U_3 + u_{21}U_1 + u_{11}U_3}{2(u_{21}u_{32} - u_{21}u_{12} - u_{11}u_{32} - u_{22}u_{31} + u_{22}u_{11} + u_{12}u_{31})}. \end{aligned} \quad (6.59)$$

Substitute (6.59) into the first and the fourth equations of (6.56), one gets

$$\begin{aligned} F(z, u_{11}, \dots, u_{43}) &= F(z, \phi, \theta, \psi) = 0, \\ G(z, u_{11}, \dots, u_{43}) &= G(z, \phi, \theta, \psi) = 0. \end{aligned} \quad (6.60)$$

From (6.60), one gets

$$\begin{aligned} \frac{\partial z}{\partial \theta} &= (F_\phi G_\theta - F_\theta G_\phi) / (F_z G_\phi - F_\phi G_z), \\ \frac{\partial z}{\partial \psi} &= (F_\phi G_\psi - F_\psi G_\phi) / (F_z G_\phi - F_\phi G_z). \end{aligned} \quad (6.61)$$

Hence,

$$\begin{aligned} \frac{\partial^2 z}{\partial \theta^2} &= \left[ (F_{\phi\theta} G_\theta + F_\phi G_{\theta\theta} - F_{\theta\theta} G_\phi - F_\theta G_{\phi\theta})(F_z G_\phi - F_\phi G_z) \right. \\ &\quad \left. - (F_\phi G_\theta - F_\theta G_\phi)(F_{z\theta} G_\phi + F_z G_{\phi\theta} - F_{\phi\theta} G_z - F_\phi G_{z\theta}) \right] \\ &\quad / (F_z G_\phi - F_\phi G_z)^2, \\ \frac{\partial^2 z}{\partial \theta \partial \psi} &= \left[ (F_{\phi\psi} G_\theta + F_\phi G_{\theta\psi} - F_{\theta\psi} G_\phi - F_\theta G_{\phi\psi})(F_z G_\phi - F_\phi G_z) \right. \\ &\quad \left. - (F_\phi G_\theta - F_\theta G_\phi)(F_{z\psi} G_\phi + F_z G_{\phi\psi} - F_{\phi\psi} G_z - F_\phi G_{z\psi}) \right] \\ &\quad / (F_z G_\phi - F_\phi G_z)^2, \\ \frac{\partial^2 z}{\partial \psi \partial \theta} &= \left[ (F_{\phi\theta} G_\psi + F_\phi G_{\psi\theta} - F_{\psi\theta} G_\phi - F_\psi G_{\phi\theta})(F_z G_\phi - F_\phi G_z) \right. \\ &\quad \left. - (F_\phi G_\psi - F_\psi G_\phi)(F_{z\theta} G_\phi + F_z G_{\phi\theta} - F_{\phi\theta} G_z - F_\phi G_{z\theta}) \right] \\ &\quad / (F_z G_\phi - F_\phi G_z)^2, \end{aligned} \quad (6.62)$$

**Table 6.6** Eigenvalues of Hessian matrices of the equilibrium configurations in Fig. 6.7

Configuration	1	2	3	4
$\lambda_1$	1.549	8.852	0.203	-0.024
$\lambda_2$	0.159	0.289	-0.499	-0.340

$$\frac{\partial^2 z}{\partial \psi^2} = [(F_{\phi\psi} G_{\psi} + F_{\phi} G_{\psi\psi} - F_{\psi\psi} G_{\phi} - F_{\psi} G_{\phi\psi})(F_z G_{\phi} - F_{\phi} G_z) - (F_{\phi} G_{\psi} - F_{\psi} G_{\phi})(F_z G_{\psi} G_{\phi} + F_z G_{\phi\psi} - F_{\phi\psi} G_z - F_{\phi} G_z \psi)] / (F_z G_{\phi} - F_{\phi} G_z)^2.$$

Equation (6.60) shows that both  $F$  and  $G$  are functions of  $(z, \phi, \theta, \psi)$ . Their derivatives with respect to  $(z, \phi, \theta, \psi)$  can be derived using the chain rule. Substituting (6.62) into (6.53), we can obtain a Hessian matrix which can be used to analyze the stability of the equilibrium configurations as shown in Fig. 6.7. Although the configuration of the payload as shown in Fig. 6.7(a) coincides with its initial configuration as shown in Fig. 6.5, this configuration is obtained by supposing that the payload is suspended with four cables. Hence, the stability analysis of this configuration can be conducted by supposing that the payload is suspended with only four relevant cables. If this configuration under this condition is stable, its corresponding initial configuration should be more stable.

For every equilibrium configuration, the positions of four relevant robots and four relevant attachment points and the center of mass as well as the orientation angles of the payload are known. Substituting all these parameters into (6.62) and then into (6.53), a Hessian matrix is available. The eigenvalues of the Hessian matrix can be easily evaluated by the package Matlab.

Table 6.6 lists the eigenvalues of the Hessian matrices of the four equilibrium configurations as shown in Fig. 6.7. From this table, it can be seen that configurations 1 and 2 are stable. But the other two configurations are unstable.

## 6.7 Conclusions

Aerial manipulation and transport with multiple aerial robots has many applications. We derived a mathematical model that captures the kinematic constraints and conditions of static equilibrium. We showed how to obtain solutions for the direct kinematics and inverse kinematics, and provided a methodology to analyze the mechanics underlying stable equilibria of the underactuated system. The application of these ideas to multi-quadrotor control and planning are discussed in [3, 13]. Experimental studies of the stability of the system are presented in [11] and conditions for uniqueness of the direct kinematics solution are established in [3].

This line of inquiry has several possible directions of future research. Clearly the general direct kinematics problem is still unsolved, even for the three robot case.

Because the system is under actuated, it is necessary to consider the dynamics of the system to determine the stability of the true dynamical system instead of merely considering the static stability. This has important implications for control. More generally, one can envision cable-actuated parallel manipulators where the anchor point is position controlled in two or three dimensions allowing the payload to be manipulated without spooling cables to change the cable length or requiring mechanical linkages directly attached to the payload.

**Acknowledgements** The authors gratefully acknowledge the support from NSF grants IIS-0413138, IIS-0427313 and IIP-0742304, ARO Grant W911NF-05-1-0219, ONR Grant N00014-08-1-0696, and ARL Grant W911NF-08-2-0004. The first author was supported in part by the PDF fellowship from the Natural Sciences and Engineering Research Council of Canada (NSERC).

## References

1. Bernard, E.: Stability of a towed body. *J. Aircr.* **35**(2), 197–205 (1998)
2. Carricato, M., Merlet, J.-P.: Direct geometrico-static problem of under-constrained cable-driven parallel robots with three cables. In: Proceedings of 2011 IEEE International Conference on Robotics and Automation (ICRA), 9–13 May 2011, pp. 3011–3017 (2011)
3. Fink, J., Michael, N., Kim, S., Kumar, V.: Planning and control for cooperative manipulation and transportation with aerial robots. *Int. J. Robot. Res.* **30**(3), 324–334 (2011)
4. Gosselin, C., Lefrançois, S., Zoso, N.: Underactuated cable-driven robots: machine, control and suspended bodies. *Adv. Intell. Soft Comput.* **83**, 311–323 (2010)
5. Gouttefarde, M., Daney, D., Merlet, J.-P.: Interval-analysis-based determination of the wrench-feasible workspace of parallel cable-driven robots. *IEEE Trans. Robot.* **5**(1), 1–13 (2010)
6. Henderson, J.F., Potjewyd, J., Ireland, B.: The dynamics of an airborne towed target system with active control. *Proc. Inst. Mech. Eng., G J. Aerosp. Eng.* **213**, 305–319 (1999)
7. Hunt, K.H.: *Kinematic Geometry of Mechanisms*. Oxford University Press, London (1978)
8. Jiang, Q., Kumar, V.: The inverse kinematics of 3-D towing. In: Proceedings of the 12th International Symposium: Advances in Robot Kinematics, Piran-Portoroz, Slovenia, June 27–July 1 (2010)
9. Jiang, Q., Kumar, V.: The inverse kinematics of cooperative transport with multiple aerial robots. Conditionally accepted by *IEEE Trans. Robot.*
10. Jiang, Q., Kumar, V.: The direct kinematics of payloads suspended from cables. In: Proceedings of the ASME 2010 International Design Engineering Technical Conferences & Computers and Information in Engineering Conference DETC2010-28036, Montreal, Quebec, Canada, August 15–18 (2010)
11. Jiang, Q., Kumar, V.: Determination and stability analysis of equilibrium configurations of payloads suspended from multiple aerial robots. *ASME J. Mech. Robot.* **4**(2), 021005 (2012)
12. Michael, N., Kim, S., Fink, J., Kumar, V.: Kinematics and statics of cooperative multi-robot aerial manipulation with cables. In: Proceedings of the ASME 2009 International Design Engineering Technical Conferences & Computers and Information in Engineering Conference, DETC2009-87677, San Diego, USA, Aug. 30–Sep. 2 (2009)
13. Michael, N., Fink, J., Kumar, V.: Cooperative manipulation and transportation with aerial robots. *Auton. Robots* **30**(1) (2011)
14. Murray, R.M.: Trajectory generation for a towed cable system using differential flatness. In: IFAC World Congress, San Francisco, CA, July (1996)
15. Oh, S.R., Agrawal, S.K.: A control Lyapunov approach for feedback control of cable-suspended robots. In: Proceedings of the IEEE International Conference on Robotics and Automation, Rome, Italy, April, pp. 4544–4549 (2007)

16. Phillips, J.: *Freedom in Machinery*, vol. 1. Cambridge University Press, Cambridge (1990)
17. Pohst, M., Zassenhaus, H.: *Algorithmic Algebraic Number Theory*. Cambridge University Press, Cambridge (1989)
18. Roth, B.: Computations in kinematics. In: Angeles, J., Hommel, G., Kovacs, P. (eds.) *Computational Kinematics*, pp. 3–14. Kluwer Academic, Dordrecht (1993)
19. Stump, E., Kumar, V.: Workspaces of cable-actuated parallel manipulators. *ASME J. Mech. Des.* **128**(1), 159–167 (2006)
20. Williams, P., Sgarioto, D., Trivailo, P.: Optimal control of an aircraft-towed flexible cable system. In: *Proceedings of the 11th Australian International Aerospace Congress*, Melbourne, Mar. 12–17, pp. 1–21 (2005)